Electrochemical and Magnetic Exchange Interactions in Trinuclear Chain Complexes Containing Oxo-Mo(V) Fragments as a Function of the Topology of the Bridging Ligand

Van Ân Ung,[†] Samantha M. Couchman,[†] John C. Jeffery,[†] Jon A. McCleverty,*[,†] Michael D. Ward,*[,†] Federico Totti,[‡] and Dante Gatteschi*[,‡]

School of Chemistry, University of Bristol, Cantock's Close, Bristol BS8 1TS, U.K., and Department of Chemistry, University of Florence, Via Maragliano 75/77, 50144 Florence, Italy

Received August 5, 1998

The trinuclear complexes [{Mo(O)(Tp*)Cl}(μ-1,*n*-$C_6H_4O_2$){Mo(O)(Tp*)}(μ-1,*n*-$C_6H_4O_2$){Mo(O)(Tp*)Cl}] (**1**, $n = 4$; **2**, $n = 3$) have been prepared [Tp* = tris(3,5-dimethylpyrazolyl)hydroborate], in which a chain of three paramagnetic oxo-Mo(V) fragments are linked by two 1,4-$[OC_6H_4O]^{2-}$ (for **1**) or 1,3-$[OC_6H_4O]^{2-}$ (for **2**) bridging ligands. The crystal structure of **1**·$(CH_2Cl_2)_{3.5}$·$(C_6H_{14})_{0.5}$ was determined: $C_{63.5}H_{88}B_3Cl_9Mo_3N_{18}O_7$; triclinic, $P\bar{1}$; $a = 12.052(2)$ Å, $b = 18.487(4)$ Å, $c = 21.039(5)$ Å; $\alpha = 68.95(2)°$, $\beta = 86.12(2)°$, $\gamma = 78.637(13)°$; $V = 4289(2)$ Å^3; $Z = 2$. It shows a V-shaped Mo−L−Mo−L−Mo array of three {(Tp*)Mo(O)} fragments with two 1,4-$[OC_6H_4O]^{2-}$ bridging ligands. The V-shape arises from the cis arrangement of the two bridging ligands at the central metal atom. Electrochemical measurements show the expected Mo(IV)/Mo(V) and Mo(V)/Mo(VI) couples at potentials consistent with significant electrochemical interactions between the terminal and central metal fragments but not between the two terminal metal fragments. Variable-temperature magnetic susceptibility measurements (1.17−225 K) show the occurrence of intramolecular antiferromagnetic (**1**) and ferromagnetic (**2**) exchange interactions between adjacent metal atoms with $J = -44.0$ (**1**) and $+4.5$ cm^{-1} (**2**) [based on $H = -J(\mathbf{S}_1\mathbf{S}_2 + \mathbf{S}_1\mathbf{S}_3)$] leading to $S = {}^1/_2$ (**1**) and ${}^3/_2$ (**2**) ground states. These results are in accord with the spin-polarization principle, which predicts that [1,4-$C_6H_4O_2$]$^{2-}$ should be an antiferromagnetic linker whereas [1,3-$C_6H_4O_2$]$^{2-}$ should be a ferromagnetic linker.

Introduction

The ability to control the sign and magnitude of the magnetic exchange interaction between adjacent metal ions in a multinuclear complex is of fundamental importance for the design and synthesis of new magnetic materials based on polymeric coordination complexes.[1−5] In most cases the magnetic interaction between magnetic centers can be rationalized by considering the overlap of their magnetic orbitals. When the interacting metal ions are sufficiently close that their magnetic orbitals overlap directly, the sign of the exchange interaction is determined by the relative symmetry of these orbitals (the Goodenough−Kanamori rules),[6−10] and polynuclear complexes with predictable magnetic properties have been prepared using this principle.[11,12] When the metal orbitals are further apart because the ions are connected by extended bridging ligands, the exchange interaction must be propagated via the orbitals of the bridging ligand, and the nature of the magnetic interaction depends in detail on the length, conformation, topology, degree of saturation, etc. of the bridging ligand. The study of how *electronic* interactions between metal centers in mixed-valence complexes vary according to the properties (length, conformation, topology, degree of saturation etc.) of the bridging ligand is well-developed, and these properties of the bridging ligand have been experimentally taken into consideration in mixed-valence complexes.[13,14] In contrast the systematic exploitation of the same features of the bridging ligands to control magnetic exchange interactions has received much less attention.[15]

We have recently determined a quantum-mechanical rationalization of the magnetic interactions between two paramagnetic oxo-Mo(V) fragments connected by 1,3- and 1,4-$[OC_6H_4O]^{2-}$ bridging ligands.[16] Density functional calculations suggest that the sign and the magnitude of the magnetic coupling, *J*, are determined by both the relative orientation of

* Corresponding author. Fax: +44 (0) 117 929 0509. E-mail: mike.ward@bristol.ac.uk.
[†] University of Bristol.
[‡] University of Florence.

(1) Kahn, O. *Molecular Magnetism*; VCH Publishers, Inc.: New York, 1993.
(2) McCusker, J. K.; Schmitt, E. A.; Hendrickson, D. N. In *Magnetic Molecular Materials*; NATO ASI Series E198; Gatteschi, D., Kahn, O., Miller, J. S., Palacio, F., (Eds.); Kluwer Academic Press: Dordrect, The Netherlands, 1991; p 297.
(3) Kahn, O.; Pei, Y.; Journaux, Y. In *Inorganic Materials*; Bruce, D. W., O'Hare, D., Eds.; Wiley: Chichester, 1992; p 59.
(4) Bushby, R. J.; Paillaud, J.-L. In *Introduction to Molecular Electronics*; Petty, M. C., Bryce, M. R., Bloor, D., Eds., Edward Arnold: London, 1995; p 72.
(5) Miller, J. S.; Epstein, A. J. *Angew. Chem., Int. Ed. Engl.* **1994**, *33*, 385.
(6) Kahn, O. *Struct. Bonding* **1987**, *68*, 89.
(7) Goodenough, J. B. *Phys. Rev.* **1955**, *100*, 564.
(8) Goodenough, J. B. *J. Phys. Chem. Solids* **1958**, *6*, 287.
(9) Kanamori, J. *J. Phys. Chem. Solids* **1959**, *10*, 87.
(10) Ginsberg, A. P. *Inorg. Chim. Acta Rev.* **1971**, *5*, 45.
(11) Gordon-Wylie, S. W.; Bominaar, E. L.; Collins, T. J.; Workman, J. M.; Claus, B. L.; Patterson, R. E.; Williams, S. A.; Conklin, B. J.; Yee, G. T.; Weintraub, S. T. *Chem. Eur. J.* **1995**, *1*, 528.
(12) Nakatani, K.; Bergerat, P.; Codjovi, E.; Mathonière, C.; Pei, Y.; Kahn, O. *Inorg. Chem.* **1991**, *30*, 3977.
(13) Ward, M. D. *Chem. Soc. Rev.* **1995**, 121.
(14) Ward, M. D. *Chem. Ind.* **1996**, 568.
(15) Lloret, F.; De Munno, G.; Julve, M.; Cano, J.; Ruiz, R.; Caneschi, A. *Angew. Chem., Int. Ed. Engl.* **1998**, *37*, 135.
(16) Bencini, A.; Gatteschi, D.; McCleverty, J. A.; Sanz, D. N.; Totti, F.; Ward, M. D. *J. Phys. Chem.*, in press.

10.1021/ic980934c CCC: $18.00
Published on Web 01/05/1999

the two paramagnetic fragments, and the substitution pattern of the bridging ligand (meta or para). However a much simpler approach based on the spin-polarization principle has been shown to be qualitatively useful. We recently demonstrated how the sign and magnitude of the magnetic exchange interaction between two paramagnetic nitrosyl-Mo(I) or oxo-Mo(V) fragments may be controlled according to the topology and conformation of the bridging ligand between them.[17−19] The key result is that a simple approach based on spin-polarization can be used to predict the sign of the magnetic exchange interaction *J*. The unpaired spin on one Mo center polarizes the spin of the electron cloud on the immediately adjacent atoms in the opposite sense: the same interaction results in an alternation of induced spin density across the bridging ligand, and ultimately determines the sign of the spin of the second unpaired electron. This principle is well-known for organic polyradicals[20−25] but has rarely been exploited in metal complexes. Thus 4,4′-bipyridine and 1,2-bis(4-pyridyl)ethene bridging ligands between {Mo^{I}(NO)(Tp*)Cl} fragments result in antiferromagnetic exchange, whereas the 3,4′-substituted isomers result in ferromagnetic exchange because the bridging pathway has changed in length by one atom.[17] Similarly, the dianion of 1,4-dihydroxybenzene as bridging ligand between {Mo^{V}(O)(Tp*)Cl} fragments affords antiferromagnetic exchange, whereas the 1,3 isomer affords ferromagnetic exchange.[18] In the trinuclear complex [{Mo(O)(Tp*)Cl}$_3$(μ-1,3,5-C_6H_3O)] the three unpaired spins are linked in a triangular array by the single bridging ligand; the meta relationship between each pair of Mo centers ensures ferromagnetic exchange to give an $S = {}^3/_2$ ground state.[18]

To test further the generality of this principle, we have now prepared and studied the two topologically linear trinuclear complexes [{Mo(O)(Tp*)Cl}(μ-1,*n*-$C_6H_4O_2$){Mo(O)(Tp*)}(μ-1,*n*-$C_6H_4O_2$){Mo(O)(Tp*)Cl}] (**1**, $n = 4$; **2**, $n = 3$; Scheme 1), containing a chain of three paramagnetic oxo-Mo(V) (d^1) fragments linked by *p*- or *m*-dihydroxybenzene bridging ligands, respectively. We describe here their syntheses and magnetic properties, and show how the simple predictive ability of the spin-polarization principle can be extended to multinuclear chains.

Experimental Section

General Details. The dinuclear complexes [{Mo(O)(Tp*)Cl}$_2$(μ-1,*n*-$C_6H_4O_2$)] ($n = 3$, 4) were prepared according to the published method.[26] The mononuclear "complex ligands" [Mo(O)(Tp*)Cl(1,*n*-OC_6H_4OH)] were isolated as byproducts from the preparations of the dinuclear complexes.[26] Instrumentation used for routine spectroscopic and electrochemical studies has been described previously.[26,27] Magnetic susceptibilities were measured in the temperature range of 1.17−255 K in an applied field of 1 T using a Metronique Ingéniérie MS03 SQUID magnetometer; diamagnetic corrections were estimated from Pascal's constants.[28,29]

Scheme 1[a]

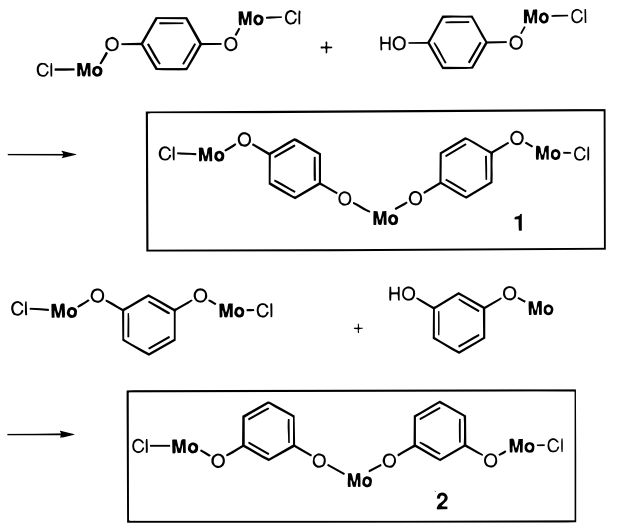

[a] **Mo** = {Mo(Tp*)O}.

Preparation of 1 and 2. To a stirred solution of [{Mo(O)(Tp*)Cl}$_2$(μ-1,n-$C_6H_4O_2$)] ($n = 4$ or 3; 0.900 g, 0.903 mmol) in dry toluene (10 cm^3) was added the appropriate mononuclear complex ligand [Mo(O)(Tp*)Cl(1,n-OC_6H_4OH)] ($n = 4$ or 3, respectively; 0.500 g, 0.903 mmol), silver acetate (0.452 g, 2.7 mmol), and sodium hydride (0.036 g, 1.5 mmol), The mixture was heated to reflux under N_2 with stirring in the dark for 24 h, and then it was evaporated to dryness *in vacuo*. The solid residue was purified by column chromatography (silica, CH_2Cl_2); the unreacted dinuclear starting material eluted first, followed by the desired trinuclear complex. Repeated chromatographic purification was often necessary to remove closely running trace impurities. The yields were 15% for **1**, 20% for **2**. In the FAB spectra of both complexes the principal peak occurred at *m*/*z* 1515 (the expected value) with the correct isotopic distribution. Elem. Anal. for **1**, found: C, 45.2; H, 5.3; N, 16.2. For **2**, found: C, 45.6; H, 5.0; N, 16.9. Required in each case for $C_{57}H_{74}B_3Cl_2Mo_3N_{18}O_7$: C, 45.2; H, 4.9; N, 16.6. IR data for **1**: $\nu_{Mo=O}$ 946, 934 cm^{-1}; ν_{B-H} 2545 cm^{-1}. For **2**: $\nu_{Mo=O}$ 948, 936 cm^{-1}; ν_{B-H} 2546 cm^{-1}.

Crystal Structure of 1·$(CH_2Cl_2)_{3.5}$·$(C_6H_{14})_{0.5}$. Dark green crystals were grown by layering hexane onto a concentrated solution of **1** in CH_2Cl_2. The crystals were very thin plates that lost solvent rapidly; the one selected (0.01 × 0.2 × 0.3 mm) was quickly coated in paraffin oil saturated with the recrystallization solvent and mounted on a Siemens SMART diffractometer under a stream of N_2 at 173 K. Crystallographic data are summarized in Table 1. In total, 29 259 reflections were collected ($2\theta_{max} = 45°$) at 173 K which, after merging, gave 11 165 independent data ($R_{int} = 0.127$). An empirical absorption correction (SADABS) was applied.[30] The structure was solved by direct methods and refined on all F^2 data using the SHELX suite of programs on a Silicon Graphics Indy computer.[31] Refinement of 620 parameters converged at R1 = 0.0876 for selected data with $I > 2\sigma(I)$; wR2 = 0.263 (all data). Hydrogen atoms were included in calculated positions and refined isotropically. Due to the weakness of the data set arising from the small crystal size, solvent loss, and disorder (both in lattice solvent molecules and between O and Cl ligands on the two terminal Mo atoms) it was not possible to perform a full anisotropic refinement. Consequently only the Mo, N, O, and Cl atoms were refined anisotropically, and the carbon atoms had to be refined with isotropic thermal parameters to keep the refinement stable.

(17) Cargill Thompson, A. M. W.; Gatteschi, D.; McCleverty, J. A.; Navas, J. A.; Rentschler, E.; Ward, M. D. *Inorg. Chem.* **1996**, *35*, 2701.
(18) Ung, V. A.; Cargill Thompson, A. M. W.; Bardwell, D. A.; Gatteschi, D.; Jeffery, J. C.; McCleverty, J. A.; Totti, F.; Ward, M. D. *Inorg. Chem.* **1997**, *36*, 3447.
(19) McCleverty, J. A.; Ward, M. D. *Acc. Chem. Res.* **1998**, *31*, 842.
(20) Karafiloglou, P. *J. Chem. Phys.* **1985**, *82*, 3728.
(21) Ovchinnikov, A. A. *Theor. Chim. Acta* **1978**, *47*, 297.
(22) Okamoto, M.; Teki, Y.; Takui, T.; Kinoshita, T.; Itoh, K. *Chem. Phys. Lett.* **1990**, *173*, 265.
(23) Takui, T.; Kita, S.; Ichikawa, S.; Teki, Y.; Kinoshita, T.; Itoh, K. *Mol. Cryst. Liq. Cryst.* **1989**, *176*, 67.
(24) Rajca, A.; Rajca, S. *J. Am. Chem. Soc.* **1996**, *118*, 8121.
(25) Minato, M.; Lahti, P. M.; van Willigen, H. *J. Am. Chem. Soc.* **1993**, *115*, 4532.
(26) Ung, V. A.; Bardwell, D. A.; Jeffery, J. C.; Maher, J. P.; McCleverty, J. A.; Ward, M. D.; Williamson, A. *Inorg. Chem.* **1996**, *35*, 5290.
(27) Amoroso, A. J.; Cargill Thompson, A. M. W.; Maher, J. P.; McCleverty, J. A.; Ward, M. D. *Inorg. Chem.* **1995**, *34*, 4828.
(28) O'Connor, C. J. *Prog. Inorg. Chem.* **1982**, *29*, 203.
(29) Carlin, R. L. *Magnetochemistry*; Springer-Verlag: New York, 1986.
(30) Sheldrick, G. M. *SADABS: A program for absorption correction with the Siemens SMART system*; University of Göttingen: Germany, 1996.
(31) *SHELXTL program system*, Version 5.03; Siemens Analytical X-ray Instruments: Madison, WI, 1995.

Table 1. Crystallographic Data for $\mathbf{1}\cdot(CH_2Cl_2)_{3.5}\cdot(C_6H_{14})_{0.5}$

empirical formula	$C_{63.5}H_{88}B_3Cl_9Mo_3N_{18}O_7$
fw	1854.82
space group	$P\bar{1}$
a, Å	12.052(2)
b, Å	18.487(4)
c, Å	21.039(5)
α, deg	68.95(2)
β, deg	86.12(2)
γ, deg	78.637(13)
V, Å^3	4289(2)
Z	2
ρ_{calc}, g cm^{-3}	1.436
μ(Mo Kα), cm^{-1}	7.69
T, °C	−100
λ, Å	0.710 73
$R1$, wR2[a,b]	0.0876, 0.2634

[a] Structure was refined on F_o^2 using all data; the value of R1 is given for comparison with older refinements based on F_o with a typical threshold of $F \geq 4\sigma(F)$. [b] $wR2 = [\sum[w(F_o^2 - F_c^2)^2]/\sum w(F_o^2)^2]^{1/2}$ where $w^{-1} = [\sigma^2(F_o^2) + (aP)^2 + bP]$ and $P = [\max(F_o^2,0) + 2F_c^2]/3$ (weighting factors are $a = 0.1160$ and $b = 0$).

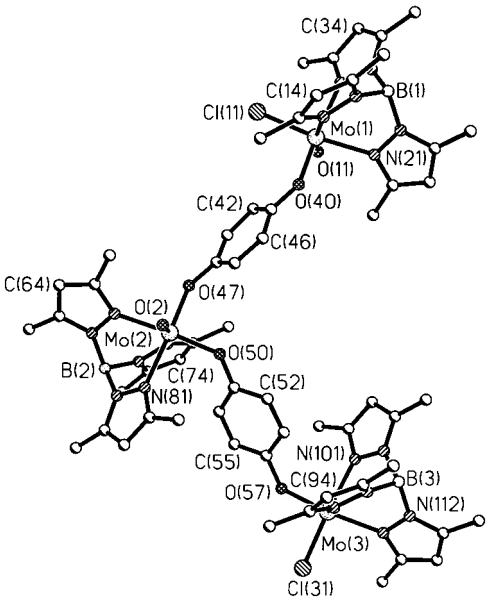

Figure 1. Crystal structure of $\mathbf{1}\cdot(CH_2Cl_2)_{3.5}\cdot(C_6H_{14})_{0.5}$.

The oxo and chloride ligands on the terminal Mo atoms [Mo(1) and Mo(3)] were mutually disordered. We have observed this before in related structures.[18,26] The weakness of the data did not allow the fractional O and Cl atoms at each site to be separated; instead the two components were restrained to have identical coordinates and thermal parameters using the restraints EXYZ and EADP from SHELX. The main component (78%) is as shown in Figure 1. The minor component (not shown, 22%) has O(11) and Cl(11) exchanged [labeled as O(12) and Cl(12) in their alternative positions], and likewise O(31) and Cl(31) are exchanged [labeled as O(32) and Cl(32) in their alternative positions]. The bond lengths involving these atoms are therefore inevitably inaccurate: the apparent Mo(1)−Cl(11) [2.290(5) Å] and Mo(3)−Cl(31) [2.266(5) Å] separations are artificially short, and the apparent Mo(1)−O(11) [1.880(8) Å] and Mo(3)−O(31) [1.883(9) Å] separations are artificially long. Bond lengths and angles involving these atoms (Table 2) should therefore be treated with caution. In addition to the trinuclear complex molecule there were three well-defined molecules of CH_2Cl_2 in the asymmetric unit. A region containing several electron-density peaks in no initially obvious arrangement was best modeled as a disordered mixture of CH_2Cl_2 and hexane (each with 50% site occupancy).

Results and Discussion

Complexes **1** and **2** were prepared in low yield (15−20%) by reaction of the dinuclear complexes $[\{Mo(O)(Tp^*)Cl\}_2(\mu\text{-}1,n\text{-}C_6H_4O_2)]$ with the appropriate mononuclear complex ligand $[Mo(O)(Tp^*)Cl(1,n\text{-}OC_6H_4OH)]$ having a pendant reactive hydroxyl group (Scheme 1). We found that addition of silver acetate to the reaction mixture improved the reactions, presumably by assisting in removal of a chloride ligand from the dinuclear complex $[\{Mo(O)(Tp^*)Cl\}_2(\mu\text{-}1,n\text{-}C_6H_4O_2)]$. Sodium hydride was used as base to deprotonate the pendant hydroxyl group of $[Mo(O)(Tp^*)Cl(1,n\text{-}OC_6H_4OH)]$. The low yields reflect both the sensitivity of the complexes to traces of moisture at elevated temperatures, and the presence of alternative reaction routes which can give metallocyclic oligomers.[32]

The complexes were characterized on the basis of their FAB mass spectra (which gave a strong molecular ion at the expected m/z value in each case) and elemental analyses. Their IR spectra also showed two closely spaced Mo═O stretching bands, consistent with the two different chemical environments of Mo. The crystal structure of **1** (Figure 1; Tables 1 and 2) provided further confirmation of the successful syntheses of the complexes. Despite the problems associated with the structural determination because of the very small crystal size and rapid solvent loss (see Experimental section) the gross structure is clear, with each metal center having a pseudo-octahedral geometry and the complex having an overall V-shape due to the cis arrangements of the two bridging ligands at the central Mo group. The metal−metal separations are Mo(1)−Mo(2), 8.8 Å; Mo(2)−Mo(3), 8.8 Å; and Mo(1)−Mo(3), 13.8 Å.

Electrochemical data (in CH_2Cl_2) are summarized in Table 3. Both complexes display two chemically reversible[33] redox processes at negative potentials, with the first wave being twice the intensity of the second (Figure 2). The former, at −1.24 V (vs Fc/Fc^+) for **1** and −1.27 V for **2**, we ascribe to the coincident Mo(V)/Mo(IV) couples of the two terminal Mo fragments which have one phenolate and one chloride ligand. The latter, at ca. −1.9 V in each case, we ascribe to the Mo(V)/Mo(IV) couple of the central Mo fragment, which has two phenolate-type ligands; the extreme negative potential is a consequence of the electrostatic interaction with the two adjacent metal fragments which are already reduced. For comparison, the Mo(V)/Mo(IV) couples of the mononuclear model complexes[34] $[Mo(O)(Tp^*)Cl(OPh)]$ (*cf.* the terminal groups of **1** and **2**) and $[Mo(O)(Tp^*)(OPh)_2]$ (*cf.* the central group of **1** and **2**) occur at −1.21 and −1.49 V vs Fc/Fc^+ respectively (measured by us under the same conditions).

At positive potentials, complex **1** shows three processes of which the first two (+0.07, +0.46 V) are chemically reversible, and the third (+1.17 V) irreversible. These are formally Mo(V)/Mo(VI) couples: the mononuclear model complexes $[Mo(O)(Tp^*)Cl(OPh)]$ and $[Mo(O)(Tp^*)(OPh)_2]$ oxidize to the Mo(VI) state at +0.68 and +0.28 V, respectively. We accordingly assign the couple at +0.07 V to the central Mo fragment

(32) Berridge, T. E.; Jones, C. J. *Polyhedron* **1997**, *16*, 3695.
(33) By "reversible" in this case we mean chemically reversible, i.e. the waves are symmetric with equal cathodic and anodic peak currents. The peak−peak separations ΔE_p are larger than the theoretical ideal, in some cases being up to 200 mV (Table 3). However, numerous spectroelectrochemical studies (Marcaccio, M.; Humphrey, E.; McCleverty, J. A.; Ward, M. D. Unpublished work) on complexes of this type (e.g. the dinuclear complexes of ref 7) have confirmed that the Mo(V)/Mo(VI) and Mo(IV)/Mo(V) couples are fully chemically reversible as long as the voltammetric waves are symmetric.
(34) Cleland, W. E., Jr.; Barhhart, K. M.; Yamanouchi, K.; Collison, D.; Mabbs, F. E.; Ortega, R. B.; Enemark, J. H. *Inorg. Chem.* **1987**, *26*, 1017.

Table 2. Selected Bond Distances (Å) and Angles (deg) for Complex **1**·$(CH_2Cl_2)_{3.5}$·$(C_6H_{14})_{0.5}$[a]

Mo(1)−O(11)	1.880(8)	Mo(2)−O(2)	1.658(9)	Mo(3)−O(31)	1.883(9)
Mo(1)−O(40)	1.952(8)	Mo(2)−O(50)	1.947(8)	Mo(3)−O(57)	1.913(8)
Mo(1)−N(31)	2.185(10)	Mo(2)−O(47)	1.953(8)	Mo(3)−N(111)	2.154(10)
Mo(1)−N(21)	2.193(11)	Mo(2)−N(61)	2.161(10)	Mo(3)−N(101)	2.187(11)
Mo(1)−Cl(11)	2.290(5)	Mo(2)−N(81)	2.176(10)	Mo(3)−Cl(31)	2.266(5)
Mo(1)−N(11)	2.328(11)	Mo(2)−N(71)	2.346(10)	Mo(3)−N(91)	2.285(11)
O(11)−Mo(1)−O(40)	99.2(4)	O(2)−Mo(2)−O(50)	103.9(4)	O(31)−Mo(3)−O(57)	101.8(3)
O(11)−Mo(1)−N(31)	93.3(4)	O(2)−Mo(2)−O(47)	101.7(4)	O(31)−Mo(3)−N(111)	92.0(4)
O(40)−Mo(1)−N(31)	166.1(4)	O(50)−Mo(2)−O(47)	90.7(3)	O(57)−Mo(3)−N(111)	165.2(4)
O(11)−Mo(1)−N(21)	92.7(4)	O(2)−Mo(2)−N(61)	91.1(4)	O(31)−Mo(3)−N(101)	94.9(4)
O(40)−Mo(1)−N(21)	88.8(4)	O(50)−Mo(2)−N(61)	164.8(4)	O(57)−Mo(3)−N(101)	90.2(4)
N(31)−Mo(1)−N(21)	84.7(4)	O(47)−Mo(2)−N(61)	88.8(4)	N(111)−Mo(3)−N(101)	83.2(4)
O(11)−Mo(1)−Cl(11)	98.9(3)	O(2)−Mo(2)−N(81)	93.1(4)	O(31)−Mo(3)−Cl(31)	95.4(3)
O(40)−Mo(1)−Cl(11)	93.2(3)	O(50)−Mo(2)−N(81)	91.2(4)	O(57)−Mo(3)−Cl(31)	91.6(3)
N(31)−Mo(1)−Cl(11)	90.7(3)	O(47)−Mo(2)−N(81)	164.1(4)	N(111)−Mo(3)−Cl(31)	92.4(3)
N(21)−Mo(1)−Cl(11)	167.8(3)	N(61)−Mo(2)−N(81)	85.3(4)	N(101)−Mo(3)−Cl(31)	168.9(3)
O(11)−Mo(1)−N(11)	171.3(4)	O(2)−Mo(2)−N(71)	169.3(4)	O(31)−Mo(3)−N(91)	173.1(4)
O(40)−Mo(1)−N(11)	84.6(4)	O(50)−Mo(2)−N(71)	85.6(3)	O(57)−Mo(3)−N(91)	84.6(4)
N(31)−Mo(1)−N(11)	82.1(4)	O(47)−Mo(2)−N(71)	82.6(4)	N(111)−Mo(3)−N(91)	81.4(4)
N(21)−Mo(1)−N(11)	79.6(4)	N(61)−Mo(2)−N(71)	79.2(4)	N(101)−Mo(3)−N(91)	82.4(4)
Cl(11)−Mo(1)−N(11)	88.7(3)	N(81)−Mo(2)−N(71)	81.8(4)	Cl(31)−Mo(3)−N(91)	86.9(3)

[a] Considering the mutual disorder of Cl(11) and O(11), and of Cl(31) and O(31), the quoted bond lengths and angles involving these atoms will be inaccurate and should be treated with caution.

Table 3. Electrochemical Data[a]

	Mo(IV)/Mo(V) couples		Mo(V)/Mo(VI) couples		
complex	terminal[b]	central[b]	terminal		central
1	−1.24 (200)[c]	−1.89 (200)	+0.46 (140)	+1.17 (i)[d]	+0.07 (140)
2	−1.27 (90)[c]	−1.85 (90)	+0.83 (i)[d]		+0.20 (90)
[Mo(O)(Tp*)Cl(OPh)]	−1.21		+0.68		
[Mo(O)(Tp*)$(OPh)_2$]		−1.49			+0.28

[a] Measurements made at a Pt-bead working electrode in CH_2Cl_2 containing 0.1 M $^nBu_4NPF_6$ as base electrolyte, with a scan rate of 0.2 V s^{-1}. Potentials are in volts vs. internal ferrocene/ferrocenium. Figures in parentheses are ΔE_p values in mV (see ref 33). [b] "Terminal" and "central" refer to the terminal {Mo(Tp*)(L)(O)Cl} and central {Mo(Tp*)$(L)_2$(O)} fragments, respectively, where L denotes one terminus of the $[OC_6H_4O]^{2-}$ bridging ligand. The potentials for the two mononuclear model complexes are listed under the heading which they most closely approximate. [c] Double-intensity wave, from coincident reduction of both terminal metal fragments. [d] *i* = irreversible process.

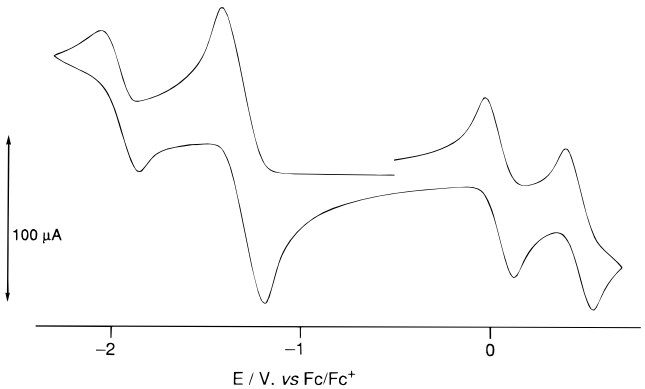

Figure 2. Cyclic voltammogram of **1** in CH_2Cl_2 (the irreversible oxidation at +1.17 V is not shown).

of **1**. However it is likely that the oxidations of **1** have some ligand-centered character, consistent with the propensity of $[1,4\text{-}C_6H_4O_2]^{2-}$ to be oxidized to 1,4-benzoquinone, so attempts to assign the oxidations to specific metal centers are of limited value.[26,35] In agreement with this complex **2**, whose 1,3-substituted bridging ligands cannot be oxidized to a quinone, shows a quite different pattern of oxidation behaviour, with just two processes apparent at +0.20 and +0.83 V of which only the first is chemically reversible. These correspond reasonably closely to the potentials of the Mo(V)/Mo(VI) couples to be expected for the central and terminal Mo fragments of **2** from the mononuclear model complexes.

The EPR spectra of both complexes are relatively uninformative. In solution at room-temperature broadened spectra were obtained (g_{iso} = 1.937) with no hyperfine coupling resolved. We observed this behavior in our earlier studies on dinuclear and trinuclear oxo-Mo(V) complexes in which the bridging ligands are relatively short.[26] The frozen solution spectra at 77 K both show very weak, featureless $\Delta m_s = 2$ transitions at half of the field (g = 3.88) of the broad $\Delta m_s = 1$ transition. We could not detect a $\Delta m_s = 3$ transition in either case.

The magnetic susceptibilities were measured in the temperature range of 1.17−255 K. The temperature dependence of the χT products of **1** and **2** are completely different from each other, showing that in **1** the coupling is dominantly antiferromagnetic, while in **2** it is ferromagnetic (Figure 3). Both compounds have a high-temperature value of χT close to 1 emu K mol^{-1}, corresponding to the limit of uncoupled spins (1.125 emu K mol^{-1} for g = 2.00). The value of χT monotonically decreases on decreasing T for **1**, reaching 0.33 emu K mol^{-1} at 2.8 K. This value is that expected for one unpaired electron. The value of χT for **2** increases on decreasing temperature reaching a maximum at 5 K (1.22 emu K mol^{-1}). Below 5 K, χT rapidly decreases to 0.44 emu K mol^{-1} at 1.17 K. This decrease at very low temperatures may be due to zero-field splitting of the ground $S = {}^3/_2$ state, to intercluster magnetic interactions, or to saturation effects.

The fits of the variable-temperature magnetic susceptibility data at temperatures down to 2 K were used to determine the

(35) Humphrey, E. R.; Marcaccio, M.; Lee, S.-M.; McCleverty, J. A.; Ward, M. D. *J. Chem. Soc., Dalton Trans.*, submitted for publication.

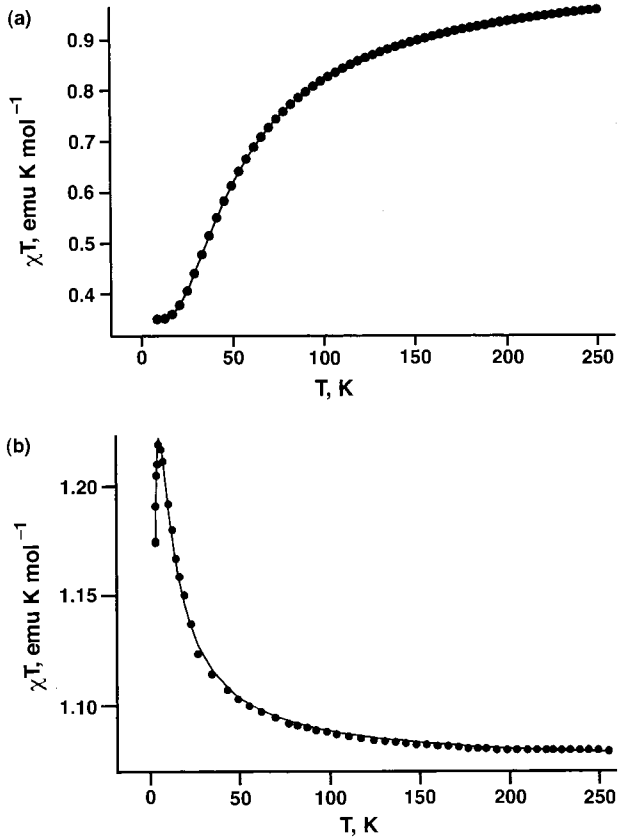

Figure 3. Magnetic susceptibility data for (a) **1** and (b) **2**. The measured data are represented by filled circles; the line through them is the computed best fit.

values of J, the exchange coupling constant between each pair of metal ions, using the exchange spin Hamiltonian in the form

$$H = -J(\mathbf{S}_1\mathbf{S}_2 + \mathbf{S}_1\mathbf{S}_3)$$

with positive J indicating ferromagnetism and negative J indicating antiferromagnetism. The molecular field approximation (MFA)[36] was applied to **2** to account for the decrease in χT below 5 K. The best fit values of J and g, and the MFA correction for **2**, are summarized in Table 4.

In **1** there is antiferromagnetic exchange between adjacent metal ions with $J = -44$ cm^{-1}, such that the ground state has $S = {}^1/_2$, which can be envisaged as a linear combination of the ↑↓↑ and ↓↑↓ spin arrangements. In this case the X-ray structure (Figure 1) shows that the two bridging pathways resemble those found for the dinuclear Mo compound with the $[1,4\text{-}C_6H_4O_2]^{2-}$ ligand, which also showed antiferromagnetic exchange.[18] In **2** there is ferromagnetic exchange between adjacent metal ions with $J = +4.5$ cm^{-1}, such that the ground state has $S = {}^3/_2$ with a ↑↑↑ arrangement of spins.

Table 4. Parameters Derived from Magnetic Susceptibility Data[a]

compound	g	J, cm^{-1}	zJ', cm^{-1} [b]
1	1.93	−44.0(3)	−
2	1.9520(4)	+4.47(5)	0.586(4)

[a] Due to the strong correlation between parameters, when errors in brackets are not given a trial-and-error approach has been used. [b] See ref 36.

The magnetic behavior of both **1** and **2** is what would be expected from the bridging ligands concerned on the basis of both the spin-polarization mechanism, which predicts that $[1,4\text{-}C_6H_4O_2]^{2-}$ should be an antiferromagnetic linker whereas $[1,3\text{-}C_6H_4O_2]^{2-}$ should be a ferromagnetic linker, and the superexchange mechanism. As we have shown for the dinuclear complexes with these bridging ligands,[16,18] the relative orientation of the metal fragments modulates the superexchange contribution, which combines with the spin-polarization contribution in determining the global J value. We note that with respect to these dinuclear complexes, the trinuclear complexes **1** and **2** have their magnetic exchange coupling constant J between adjacent metal centers approximately halved: −80 vs −44 cm^{-1} with 1,4-$[OC_6H_4O]^{2-}$ as bridging ligand, and +9.8 vs +4.5 cm^{-1} with 1,3-$[OC_6H_4O]^{2-}$ as bridging ligand. This may simply be due to the fact that the central metal ion has a different ligand donor set than the two terminal ones. Thus the antiferromagnetic coupling of −80 cm^{-1} in $[\{Mo(Tp^*)(O)Cl\}_2(\mu\text{-}1,4\text{-}OC_6H_4)]$ is between two equivalent $\{Mo(Tp^*)(O)Cl(OAr)\}$ fragments,[18] whereas the reduced coupling of −44 cm^{-1} in **1** is between one $\{Mo(Tp^*)(O)Cl(OAr)\}$ fragment and one $\{Mo(Tp^*)(O)(OAr)_2\}$ fragment. Direct comparisons of the J values in the dinuclear and trinuclear complexes are therefore not appropriate.

In conclusion, it appears therefore that the predictive value of the spin-polarization mechanism extends to linear trinuclear complexes as well as triangular and dinuclear complexes.[18]

Acknowledgment. We thank the EPSRC for studentships (V.A.U. and S.M.C.).

Supporting Information Available: One X-ray crystallographic file, in CIF format, is available on the Internet only. Access information is given on any current masthead page.

(36) Ginsberg, A. P.; Lines, M. E. *Inorg. Chem.* **1972**, *11*, 2289.

IC980934C